Supporting information

Photothermally Triggered Silk Fibroin Microneedles with Coordinated Gallic Acid–Iron Networks for Synergistic Infected Burn Wound Therapy

Wang Sun[a,b,†], Rui Xu[a,†], Wenshuya Li[c,†], Ziyan Chen[a], Mengting Yin[d], Haibo Liu[d], Feng Chen[a,b,d,*], Haijian Ni[a,*] and Xinyu Zhao[a,*]

[a]Center for Orthopaedic Science and Translational Medicine, Department of Orthopaedics, Shanghai Tenth People's Hospital, School of Medicine, Tongji University, Shanghai, 200072, PR China

[b]Suzhou First People's Hospital, School of Medicine, Anhui University of Science and Technology, Anhui, 234000, PR China

[c]Department of Plastic Surgery, The Second Hospital of Hebei Medical University, Shijiazhuang, Hebei, P. R. China

[d]Shanghai Key Laboratory of Craniomaxillofacial Development and Diseases, Shanghai Stomatological Hospital & School of Stomatology, Fudan University, Shanghai, PR China

*Corresponding author.

E-mail addresses: xyzhao@tongji.edu.cn (X. Zhao), nihaijianch@163.com (H. Ni), chen_feng@fudan.edu.cn (F. Chen)

†Authors contributed equally.

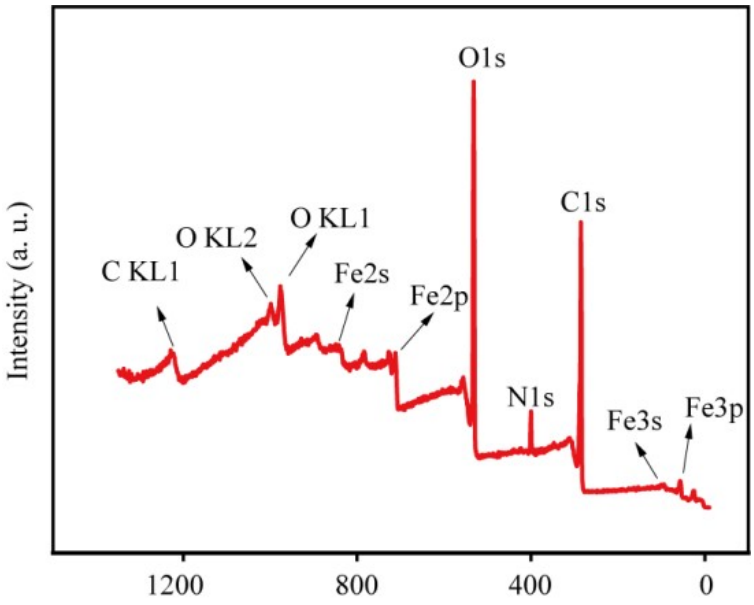

Figure S1. XPS spectrum of GFe@SFMSs.

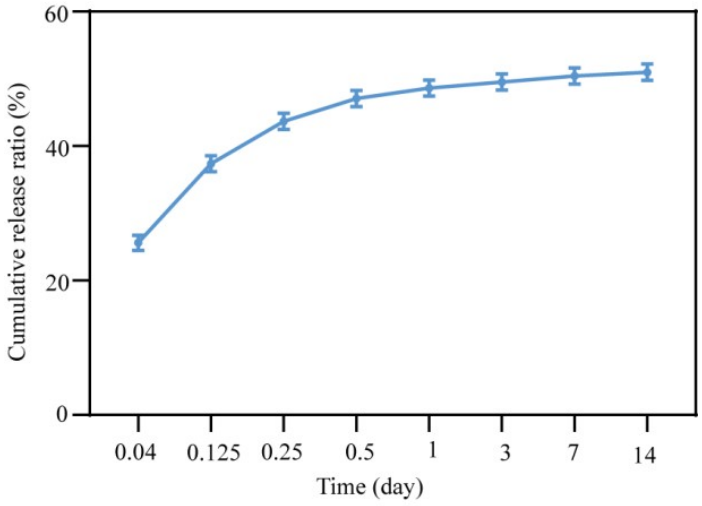

Figure S2. The cumulative release rate of iron from GFe@SFMSs at different time points.

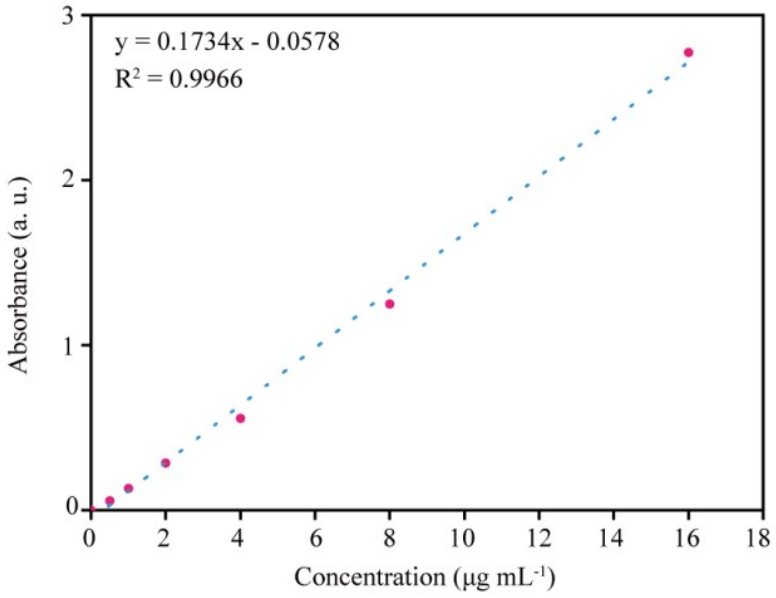

Figure S3. The calibration curve correlating the UV absorption peak of Rhodamine B with its concentration.

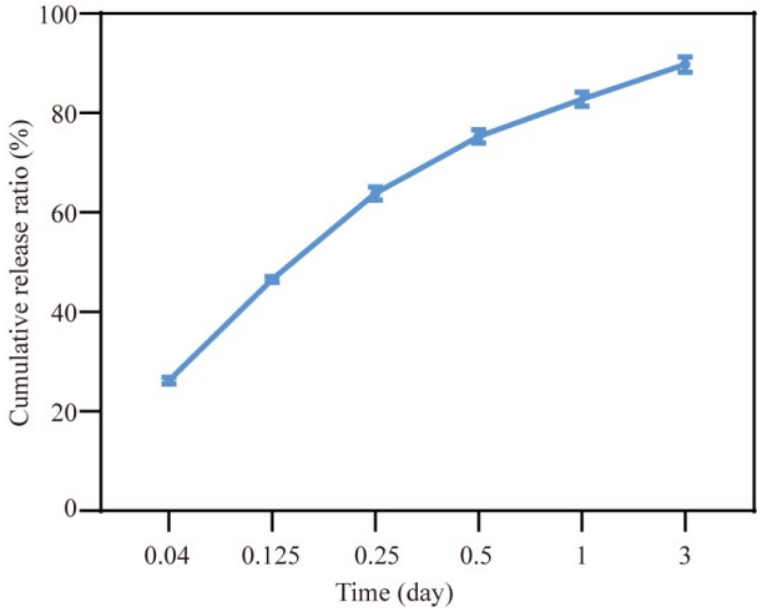

Figure S4. The cumulative release rate of Rhodamine B from MN at different time points.

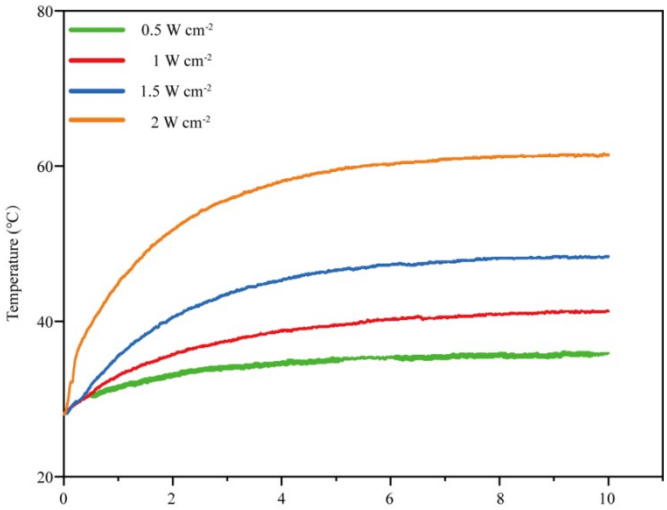

Figure S5. Photothermal heating curves of GFe@SFMSs solution under the 808 nm irradiation with different laser powers.

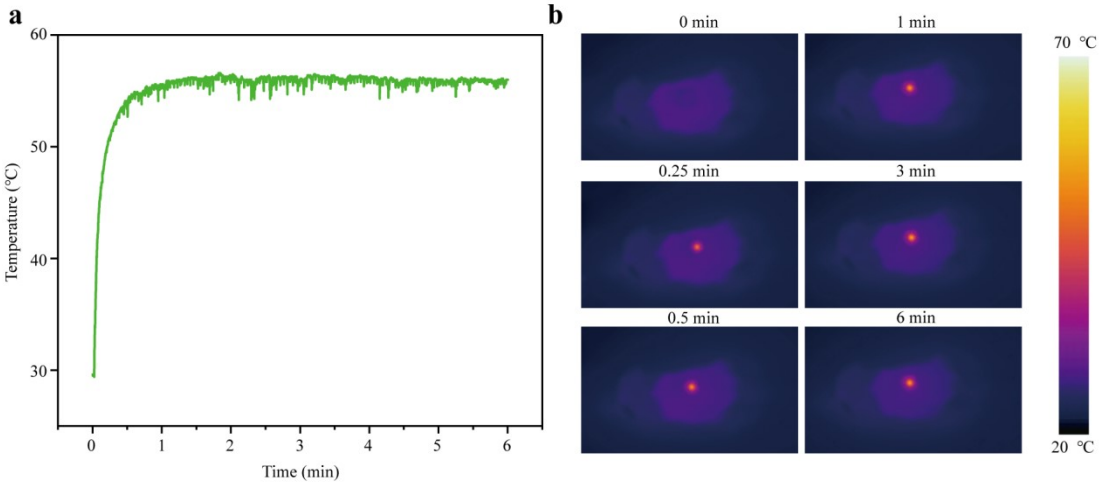

Figure S6. Photothermal heating curves GFS-MN under the NIR irradiation (808 nm, 1.0 W cm^{-2}) were obtained *in vivo* in mice. (b) Photothermal images of GFS-MN with the NIR irradiation (808 nm, 1.0 W cm^{-2}) for 6 min were captured *in vivo* in mice.

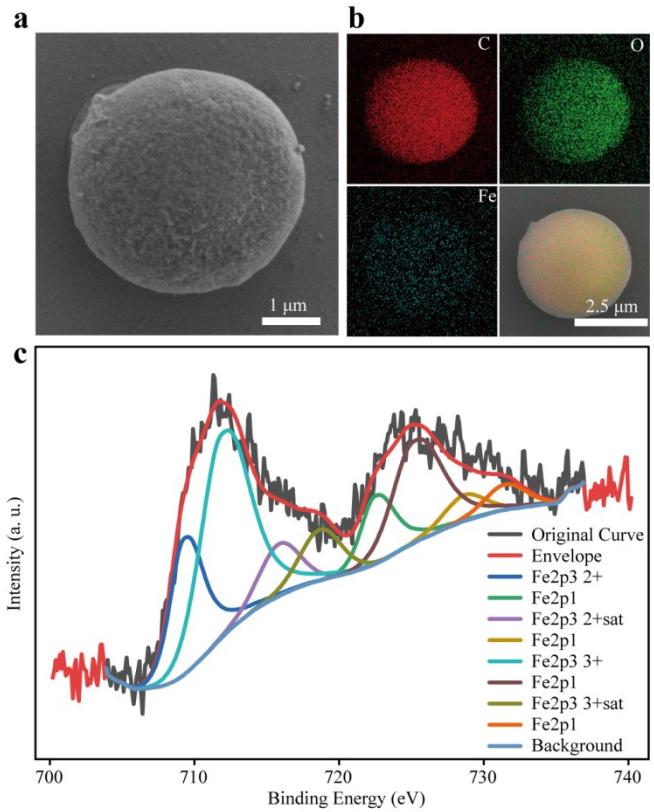

Figure S7. The characterization of GFe@SFMSs after photothermal treatment (808 nm, 1 W cm^{-2}, 10 min): (a) SEM image (Scale bar: 1 μm). (b) EDS analysis (Scale bars: 2.5 μm). (c) XPS spectra.

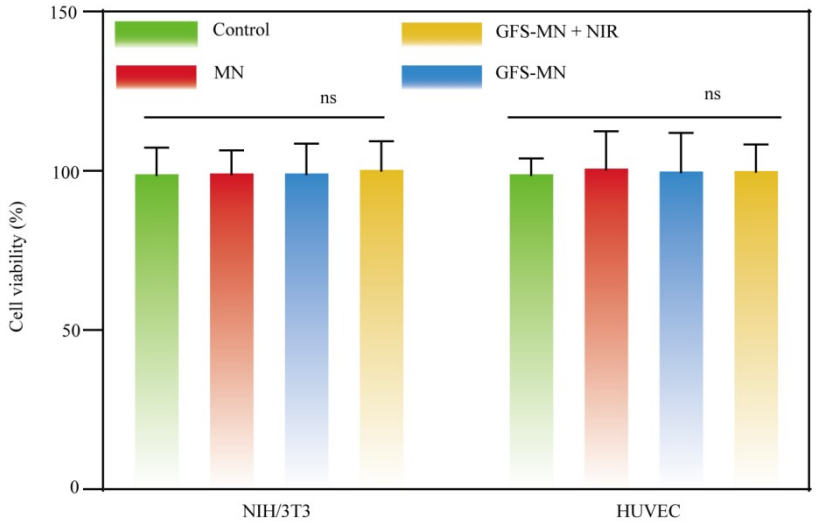

Figure S8. Cytotoxicity assays were performed on different groups using NIH/3T3 and HUVEC cells.

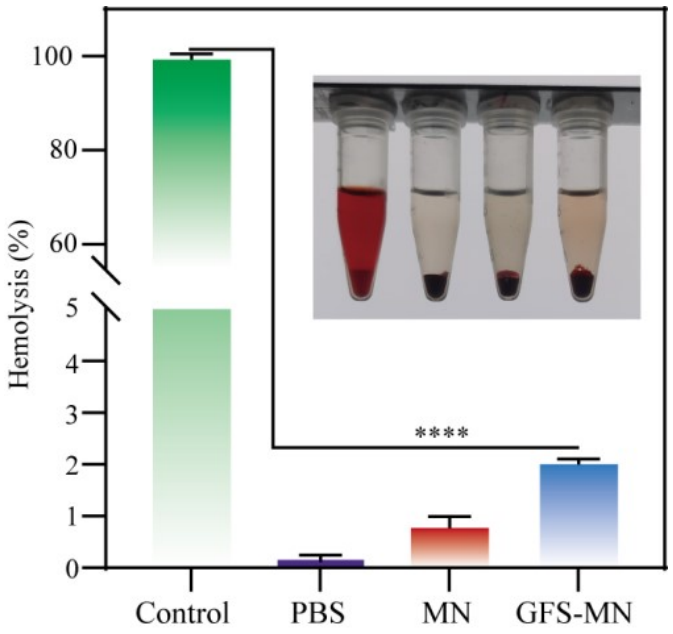

Figure S9. Hemolysis characteristic of rat blood treated with different groups (n = 3). PBS and water are used as a negative and positive control.

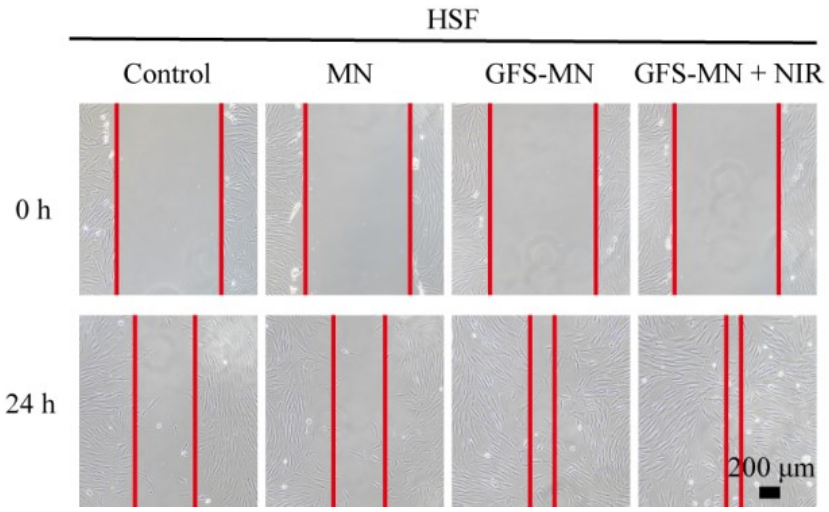

Figure S10. Images of wound scratch healing assay for HSF (Human Skin Fibroblast) cells.

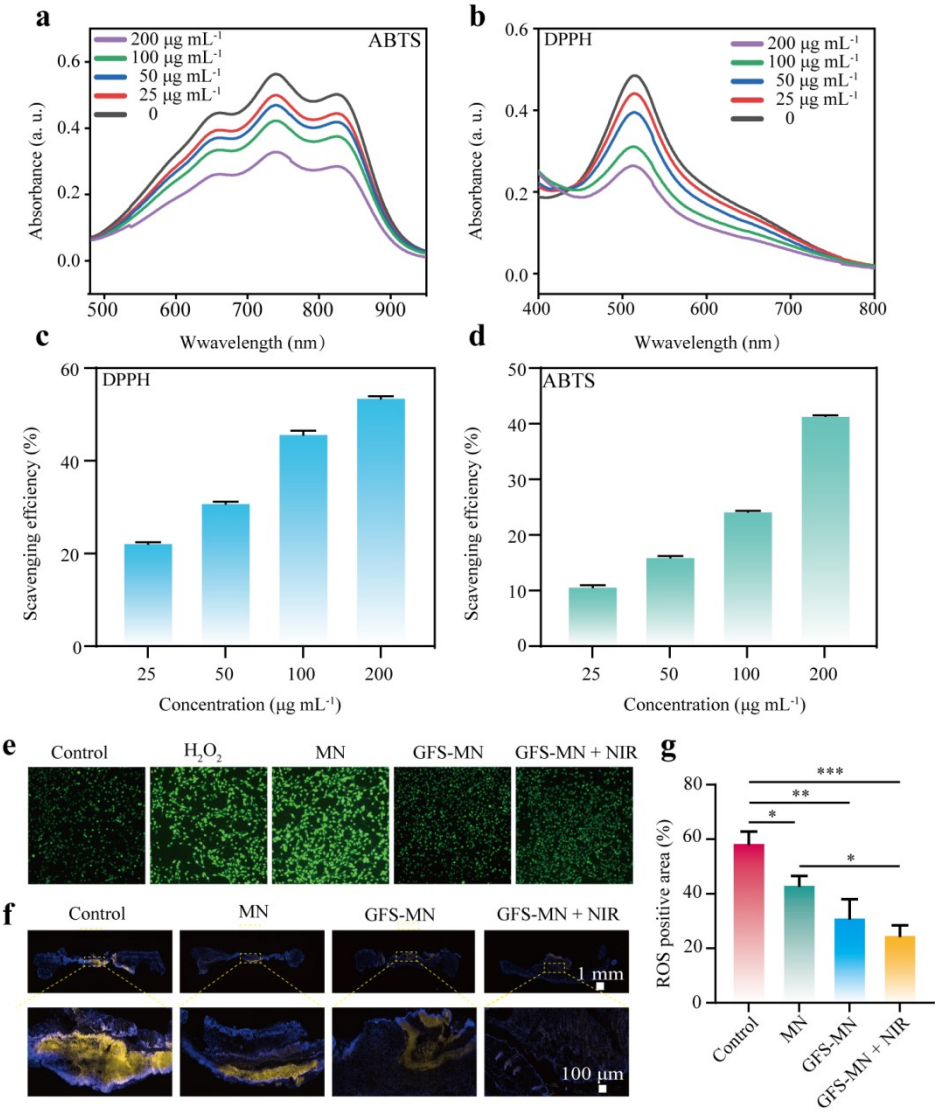

Figure S11. Antioxidant properties of the GFS-MN in scavenging free radicals and ROS: (a-d) Absorbance curves and ability of different concentrations of GFe@SFMSs to scavenge different free radicals: (a,d) ABTS, (b,c) DPPH. (e) Fluorescent photographs of ROS levels in NIH/3T3. (f) Representative images of wound tissue sections in different groups stained by ROS on day 7. (g) Quantitative analysis of fluorescent images of ROS in wound tissue sections from different groups on day 7.

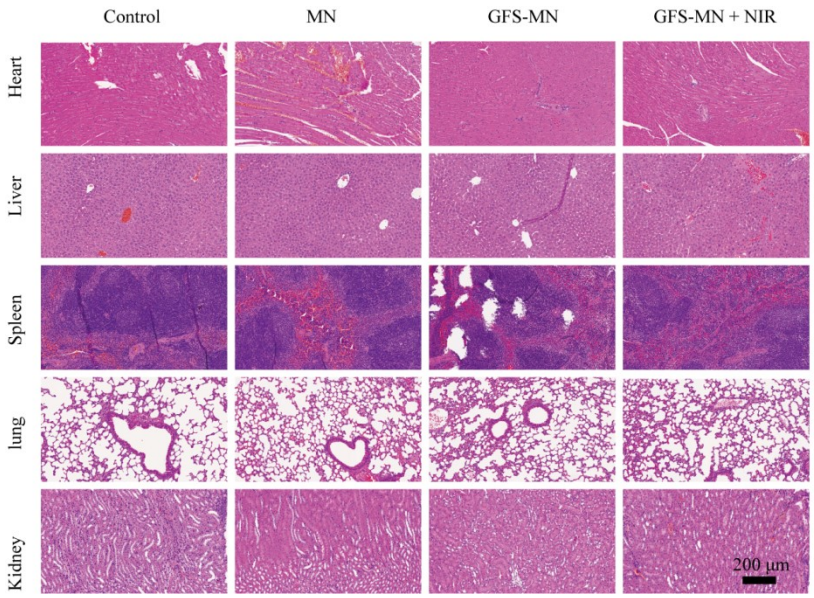

Figure S12. Representative images of heart, liver, spleen, lung, and kidney sections from different groups stained by H&E on day 14. Scale bar: 200 μm.